

Report for exercise 4 from group H

Tasks addressed: 5

Authors:

Antonia Gobillard ()
 Nayeon Ahn ()
 Muhammed Yusuf Mermmer ()
 Milena Schwarz ()
 Hammad Basit ()

Last compiled:

2024-05-18

Source code:

https://github.com/Hammad-7/MLCMS_Exercises.git

The work on tasks was divided in the following way:

Antonia Gobillard () Project lead	Task 1	20%
	Task 2	20%
	Task 3	20%
	Task 4	20%
	Task 5	20%
Nayeon Ahn ()	Task 1	20%
	Task 2	20%
	Task 3	20%
	Task 4	20%
	Task 5	20%
Muhammed Yusuf Mermmer ()	Task 1	20%
	Task 2	20%
	Task 3	20%
	Task 4	20%
	Task 5	20%
Milena Schwarz ()	Task 1	20%
	Task 2	20%
	Task 3	20%
	Task 4	20%
	Task 5	20%
Hammad Basit ()	Task 1	20%
	Task 2	20%
	Task 3	20%
	Task 4	20%
	Task 5	20%

Report on task 1, Vector fields, orbits, and visualization

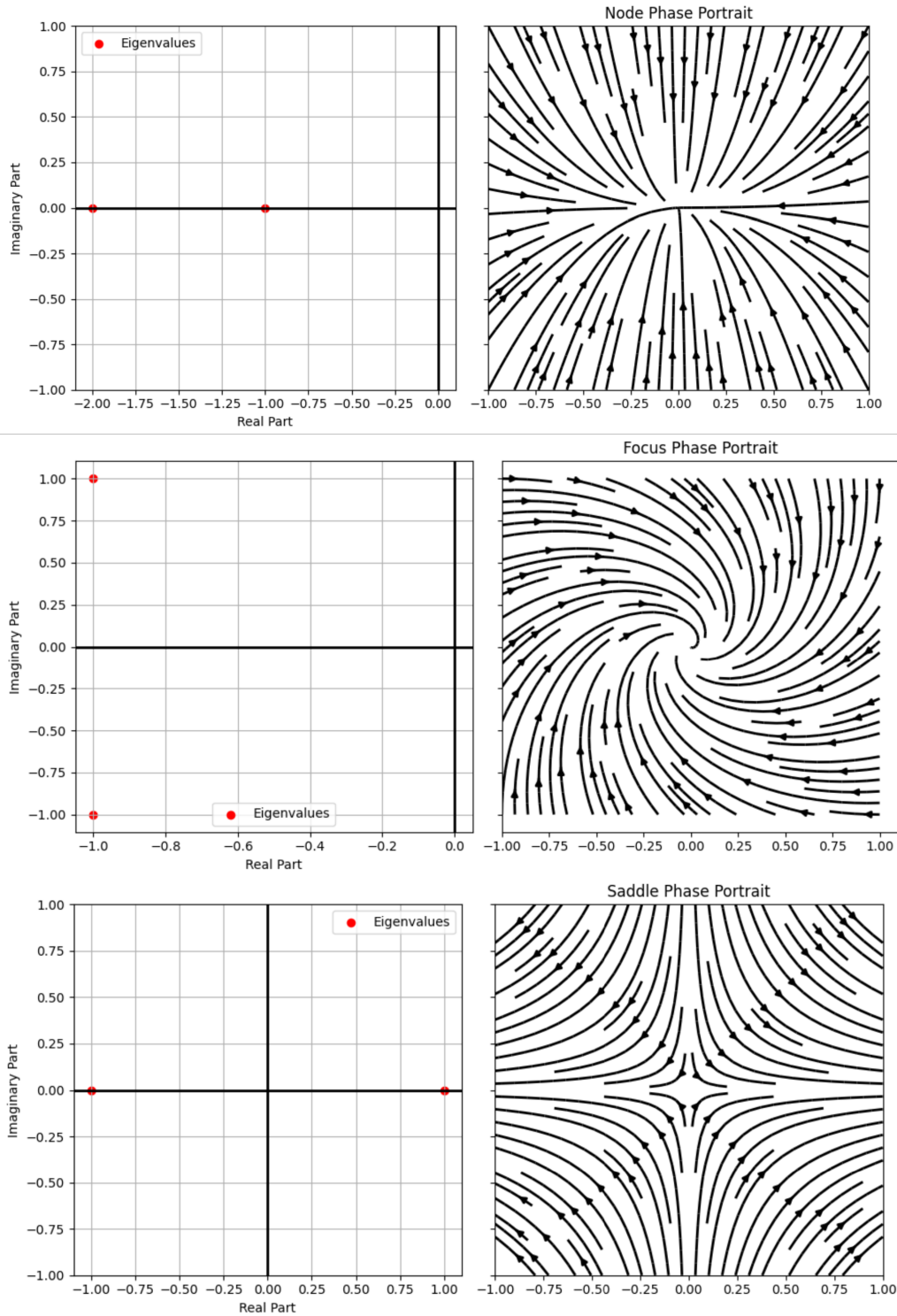


Figure 1: Phase portraits depending on the eigenvalues of the parametrized matrix

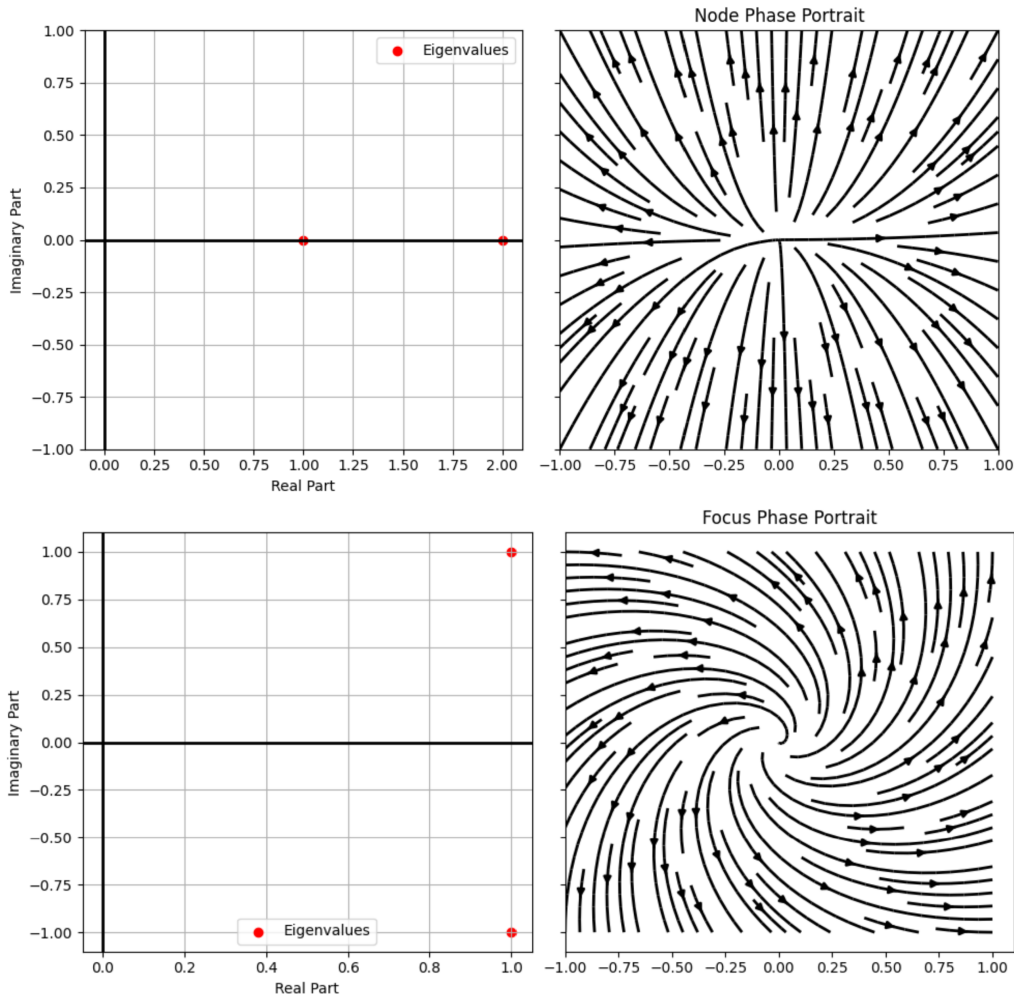


Figure 1: Phase portraits depending on the eigenvalues of the parametrized matrix

The first task of exercise 4 asks to construct a figure similar to Fig. 2.5 in the book of Kuznetsov [5]. The figure shows a connection between eigenvalues and their corresponding phase portraits. To plot the phase portraits, we utilised the `streamplot` functionality of `matplotlib` [2].

The following matrices were used (table 1):

Eigenvalues	Matrix	Phase Portrait
2 real negative	$\begin{pmatrix} -1 & 0 \\ 0 & -2 \end{pmatrix}$	Node (stable)
conjugate complex negative	$\begin{pmatrix} -1 & 1 \\ -1 & -1 \end{pmatrix}$	Focus (stable)
2 real: 1 positive, 1 negative	$\begin{pmatrix} +1 & 0 \\ 0 & -1 \end{pmatrix}$	Saddle (unstable)
2 real positive	$\begin{pmatrix} +1 & 0 \\ 0 & +2 \end{pmatrix}$	Node (unstable)
conjugate complex positive	$\begin{pmatrix} +1 & -1 \\ +1 & +1 \end{pmatrix}$	Focus (unstable)

Table 1: Eigenvalues, matrices and their resulting phase portraits

The stable portraits can be turned into unstable ones and vice versa by changing all the signs within the

matrix. The corresponding phase portraits differ in direction only.

Besides the phase portraits, the eigenvalues were also plotted. First, they were calculated using the `eig` function of `Numpy` [1] and afterward plotted via the function `scatter` of `matplotlib`. The resulting graphics are depicted in figure 1.

These systems are not equivalent orbitally or smoothly. However, the orbits can be mapped onto the ones of the next system using a homeomorphism $h : U \rightarrow U$ which is continuous and invertible. This makes the systems topologically equivalent within U .

Report on task 2, Common bifurcations in nonlinear systems

In examining the influence of α on the roots of the equation 6 ($\alpha - x^2$) and equation 7 ($\alpha - 2x^3 - 3$), we implemented the function `plot_bifurcation_diagram`. This function begins by generating an α spectrum based on specified initial and endpoints, along with the desired number of data points, utilizing `numpy`'s `linspace` function.

Subsequently, within the for loop iterating over `alpha_values`, the functions `equation6` and `equation7` come into play. The return values of these functions are systematically filled with corresponding α values. Leveraging `numpy`'s `roots` method, we ascertain the roots of the polynomial list derived from these functions.

The resultant root values are then employed to construct a comprehensive graph. Here, the x-axis delineates α values, while the y-axis represents the corresponding Steady States' values. For a visual representation, refer to Figure 2.

To enhance the interpretability of the graph in terms of stability, we introduced distinctive blue and red points along the x-axis. Blue points indicate the presence of roots, signaling stability in the system. Conversely, red points highlight the absence of roots, pointing towards instability for the associated α values in equations 6 and 7. This visual aid provides a clear delineation of stability patterns across the parameter space.

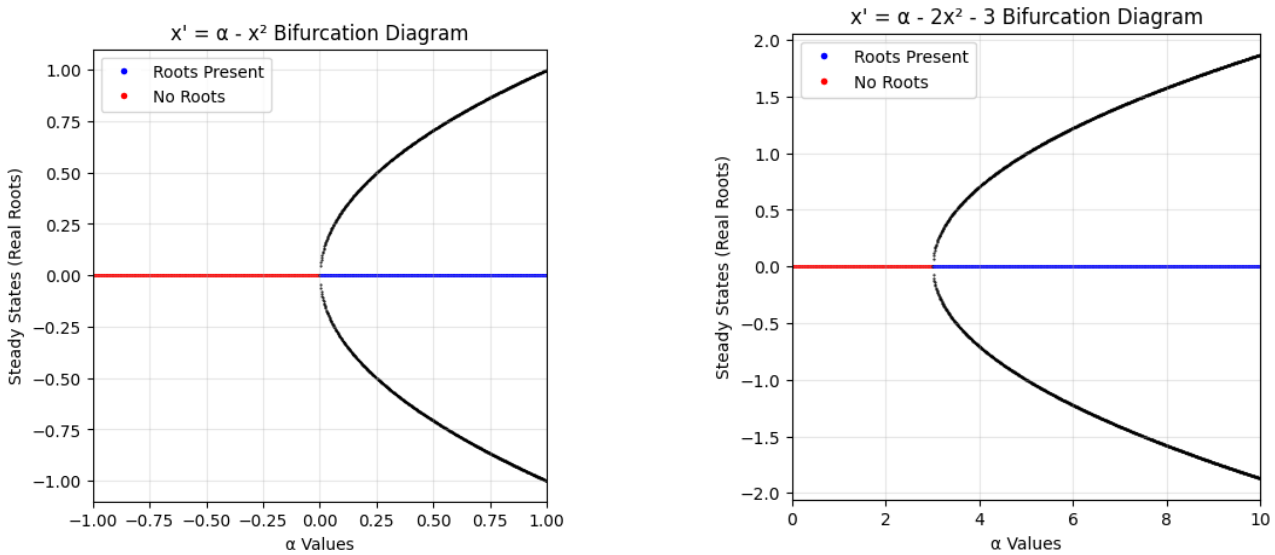


Figure 2: Bifurcation Diagrams of $x' = \alpha - x^2$ and $x' = \alpha - 2x^3 - 3$

In examining equation 7, the initial threshold range of -1 to 1 proved insufficient, prompting an extension of the interval to 0 to 10 for a more comprehensive investigation. The analysis involved a total of 1001 points for both equations 6 and 7, ranging from +1 to 1000. This broad range was purposely chosen to gain a thorough understanding of the system's behavior, with a specific focus on the pivotal middle point (0) of the steady state.

Concerning equation 6, a key observation is that points greater than 0 consistently yield two real roots. Conversely, for points smaller than 0, real roots are not feasible due to the inherent impossibility of a square of a real number being equal to a negative value in real systems.

Taking a deeper dive into the analysis, at the critical 0 point, a **saddle-node bifurcation** occurs. This intriguing phenomenon signifies the collision and subsequent annihilation of two fixed points within the dynam-

ical system. The manifestation is visually depicted by a small black point, acting as a clear separator between the blue and red lines on the graph, with a singular root located at (0,0).

Additionally, it's noteworthy that the density of points around 0 is noticeably reduced. This phenomenon can be attributed to the heightened sensitivity of root values to slight variations in α . The system undergoes rapid and significant alterations in the root values with minor changes in α , resulting in an elongated α interval around the zero point. This observation underscores the intricate dynamics of the system, highlighting its responsiveness to subtle fluctuations in parameter values.

Observing the bifurcation diagram for equation 7 reveals a parallel occurrence to equation 6, albeit in distinct regions. Notably, for equation 7, the point density diminishes as we approach $\alpha = 3$. No points exist for α values smaller than 3, while there are consistently two points for values greater than 3. The bifurcation type observed in this scenario is also identified as a **saddle-node bifurcation**.

Beyond the visual similarity in the diagrams, a more explicit connection between equation 6 and equation 7 can be established. Both equations are 2nd-order polynomials, with equation 7 exhibiting a 3-unit delay to the right and a narrower profile due to the coefficient of 2 for x^2 . This relationship allows us to explicitly demonstrate that equation 6 can be mapped to equation 7 (or vice versa) through a combination of delay and multiplication. Consequently, we can assert that these two equations share the **same normal form**.

The **topological equivalence** of these two equations is notable at the point $\alpha = -1$, where both equations share the absence of steady states, placing them in the same dynamical situation. However, this equivalence breaks down at $\alpha = 1$. At this juncture, equation 6 features 2 steady states, while equation 7 continues to lack any steady states. This distinction highlights the sensitivity of the system's behavior to changes in the parameter α , leading to divergent dynamics at different values of α .

Report on task 3, Bifurcations in higher dimensions

We first analyze the Andronov-Hopf bifurcation occurring for a system with one parameter α in a two-dimensional state space having:

$$\begin{aligned}\dot{x}_1 &= \alpha x_1 - x_2 - x_1(x_1^2 + x_2^2) \\ \dot{x}_2 &= x_1 + \alpha x_2 - x_2(x_1^2 + x_2^2)\end{aligned}$$

We plot three phase diagrams of the bifurcation with different values for α as reported in the table underneath (table 2):

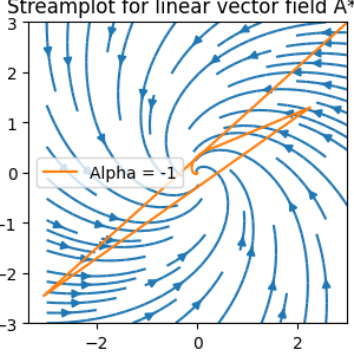
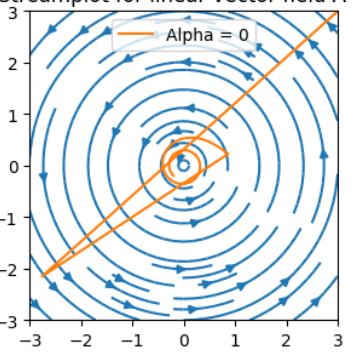
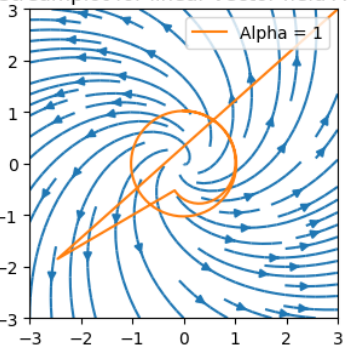
Value of α	Visualization of the Phase Diagram	Observations
-1		<p>Trajectories spiral inward around the equilibrium at the origin. The equilibrium is asymptotically stable.</p>
0		<p>Trajectories neither converge nor diverge. They form loops around the equilibrium at the origin. The equilibrium is asymptotically "weakly" stable.</p>
1		<p>Trajectories spiral outward and diverge from the equilibrium at the origin. The system is unstable.</p>

Table 2: Observations of Phase Diagrams for Different α Values

Let's now visualize two orbits of the system, for $\alpha = 1$ forward in time, one starting at the point $(2, 0)$ and the other at $(0.5, 0)$. To do so, we used Euler's method with a step size 10 times smaller by defining the time range as `time = np.linspace(0, 100, 10000)` instead of `np.linspace(0, 10, 100)`.

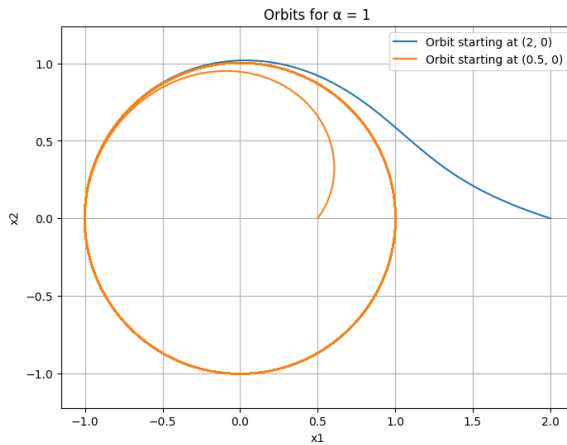


Figure 3: Two orbits of the system with $\alpha = 0$ for 2 different origins

The cusp bifurcation occurs for a system with two parameters $\alpha = (\alpha_1, \alpha_2)$ in a one-dimensional state space having:

$$\dot{x} = \alpha_1 + \alpha_2 x - x^3$$

We visualize the bifurcation surface (i.e. all points (x, α_1, α_2) where $\dot{x} = 0$) in a 3D plot with α_1 and α_2 on the bottom plane and x in the third direction. To do so we sample points (x, α_2) uniformly and then plot the so-called cusp surface as a function α_1 of (x, α_2) .

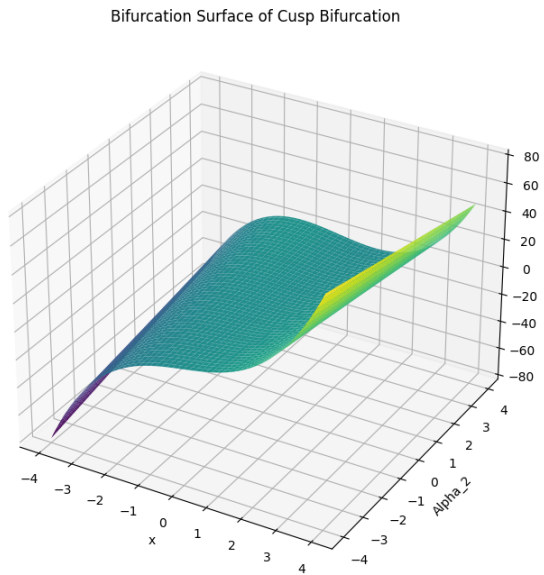


Figure 4: 3D plot of the cusp bifurcation

As shown in the 3D plot, the name of the bifurcation must come from its characteristic shape as it highlights a sudden qualitative change in the behavior of the system. There is a sort of a threshold value of α , really noticeable on the visualization, which marks the change.

Report on task 4, Chaotic dynamics

Now, our goal is to study chaos in dynamical systems using two systems.

Part 1: For this part, we focus on a very simple equation of "logistic map" given by the equation (1) where x is the current state, r is the growth rate, and x_{n+1} is the next state with $x \in [0, 1]$ and $r \in (0, 4]$

$$x_{n+1} = rx_n(1 - x_n), \quad n \in \mathbb{N} \quad (1)$$

- **Vary r from 0 to 2:** For this task, we plotted the logistic map for four different values of $x = [0.25, 0.5, 0.75, 0.9]$ and r values between 0 and 2 with 0.1 increments on 50 timesteps. Figure 5 shows two outputs of a logistic map for different values of r and x . Looking at these plots closely, we can see that for values of r below 1, the steady state gets down to zero or dies out. We can look at this with the analogy of x being the rabbit population and r being the reproduction rate. So, if the reproduction rate is too low ($r < 1$), the rabbit population dies out as can be seen in figure 5a. But if the reproduction rate is higher ($1 < r < 2$), the population reaches a constant value (not zero) or there is no change in the population and the rate of death is equal to the rate of birth as can be seen in figure 5b. The population either increases or decreases ($x=0.5, r=1.4$) but reaches a constant steady state.

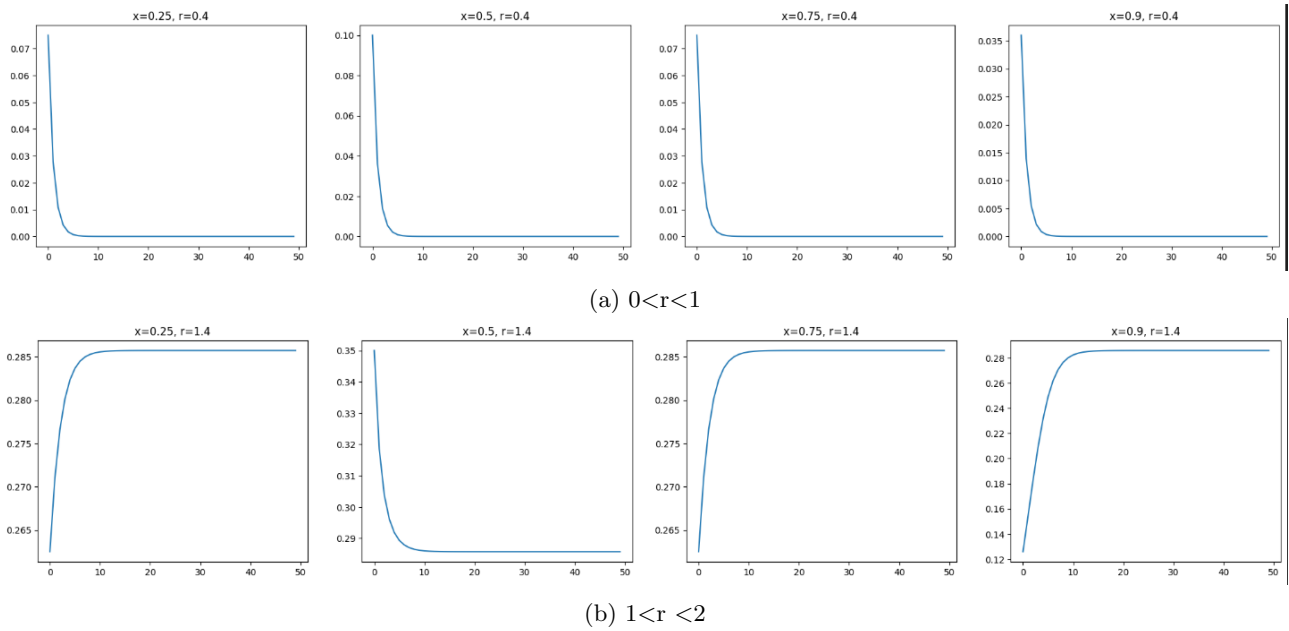


Figure 5: Logistic map for different values of r and x

We can observe the same in the bifurcation diagram 6. For r values below 1, the function dies out or becomes 0, while for r values between 0 and 1, the function has a constant not zero value. Also, there are no bifurcations in this range of r .

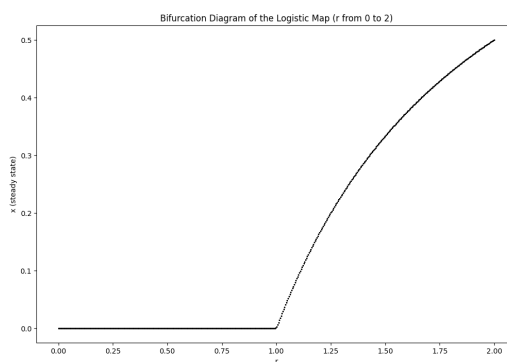


Figure 6: Bifurcation Diagram for r between 0 and 2

- **Vary r from 2 to 4:** We repeat the same experiment for r values between 2 to 4 and observe the results. We use the same four different values of $x = [0.25, 0.5, 0.75, 0.9]$ and plotted the logistic map for 100 timesteps. Figure 7 shows three outputs of the logistic map for different values of r and x. We can observe the changes in these figures now. For the r value between 2 and 3 as shown in figure 7a, the population first fluctuates before becoming constant (not zero). For r values between 3 and roughly 3.5, as shown in figure 7b, the population permanently oscillates between two values. Here, we can say that a bifurcation has occurred. If we keep increasing r and look at the graph after 3.5 as seen in figure 7c (here for r=3.6), the graph starts oscillating rapidly between multiple values. We can now say that the values are pseudo-random (as it is deterministic) or, in other terms, that chaos has ensued.

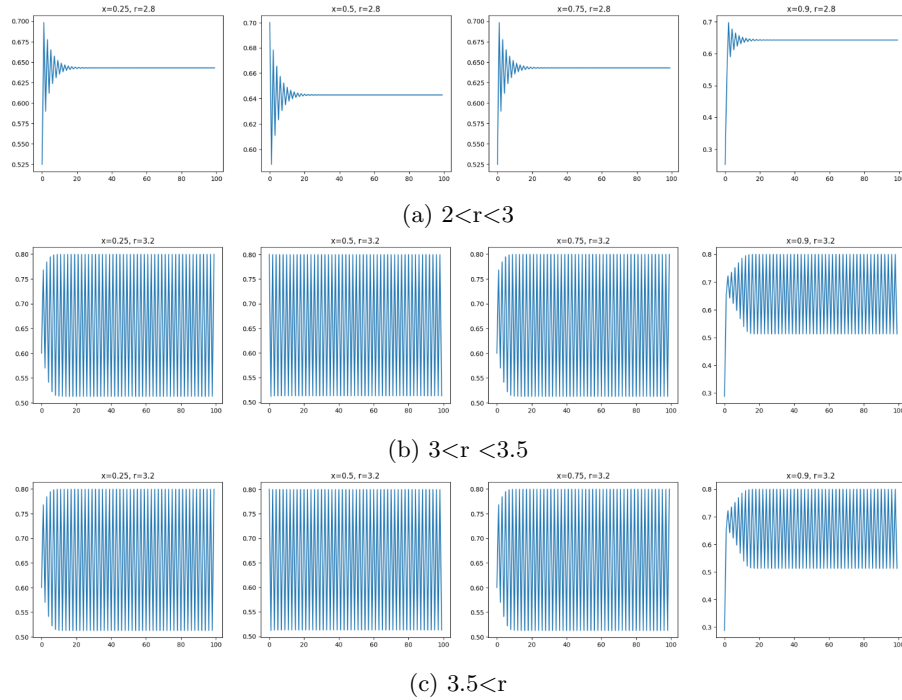
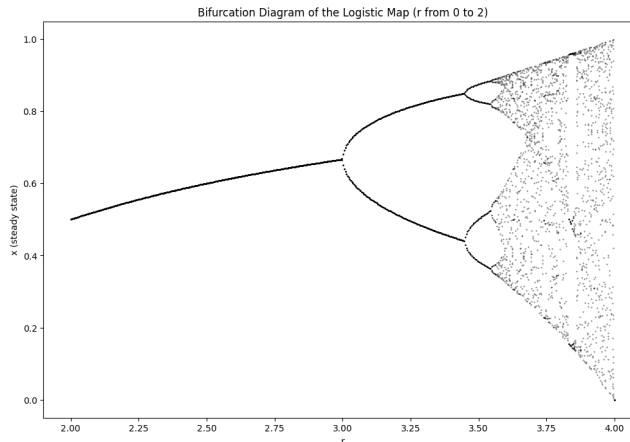


Figure 7: Logistic map for different values of r and x

We can observe the same in the bifurcation diagram 8. For values between 2 and 3, we only see one steady state. As the r value increases beyond 3, the steady state bifurcates into two. Increasing r further beyond 3.5, it further bifurcates into 4 values, and then rapidly into 8, 16, 32, etc. We can say that the values are now chaotic and pseudo-random.

Figure 8: Bifurcation Diagram for r between 2 and 4

- **Bifurcation diagram between 0 and 4:** We plotted the bifurcation diagram for $x=0.5$ for r values between 0 and 4, as shown in Figure 9. We utilized the function `plot_bifurcation_diagram` in `utils.py` to generate the bifurcation diagrams for this part and the previous two sections. To observe the final state of the system, we ran the logistic map for a specific number of timesteps to get rid of transient values and selected only the last few values (steady state) for plotting. We can again see that for r values between 0 and 1, we get 0 as the steady state, for values between 1 and 3, we can see a non-zero steady state, after 3, the graph bifurcates into two values. Increasing r beyond 3.5, the values bifurcate continuously into 4, 8, 16, etc. We can say that the values are now chaotic. One of the interesting observations that can be seen in the graph is that for r values roughly around 3.8, the graph shows non-chaotic behaviour with steady state oscillating between 3 distinct values. But with a further increase in r , the steady state again becomes chaotic.

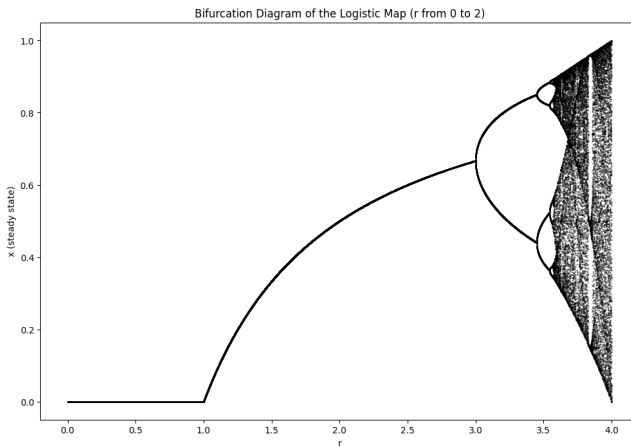


Figure 9: Bifurcation Diagram for r between 0 and 4

Part 2: For this part, we continue our exploration of chaotic dynamics using another famous attractor known as the Lorenz attractor [3], which is a strange attractor with chaotic dynamics. The system is represented by the following equations which we implemented in the function `lorenz_system()`:

$$\frac{dx}{dt} = \sigma(y - x) \quad (2)$$

$$\frac{dy}{dt} = x(\rho - z) - y \quad (3)$$

$$\frac{dz}{dt} = xy - \beta z \quad (4)$$

- **$\mathbf{X}_0 = [10, 10, 10]$:**

We visualize the trajectory of the Lorenz system by simulating its evolution from an initial state $\mathbf{X}_0 = [10, 10, 10]$ throughout $T_{\text{end}} = 1000$ units of time. The simulation is performed with a timestep of 0.01, and the system parameters are set to $\sigma = 10$, $\beta = \frac{8}{3}$, and $\rho = 28$. The trajectory can be seen in figure 10a which is like a path the system takes. Each dot on the path represents a single moment in time, recorded every 0.01 seconds. The figure also shows where the system starts and where it ends. Looking closely at the trajectory, we notice that no values are repeated and the system follows a unique path without ever going back to where it has been before. It's a chaotic diagram but deterministic. This is one of the most important observations as one can conclude that no two systems starting from two different points will ever follow each other. This will be more apparent in our next experiment.

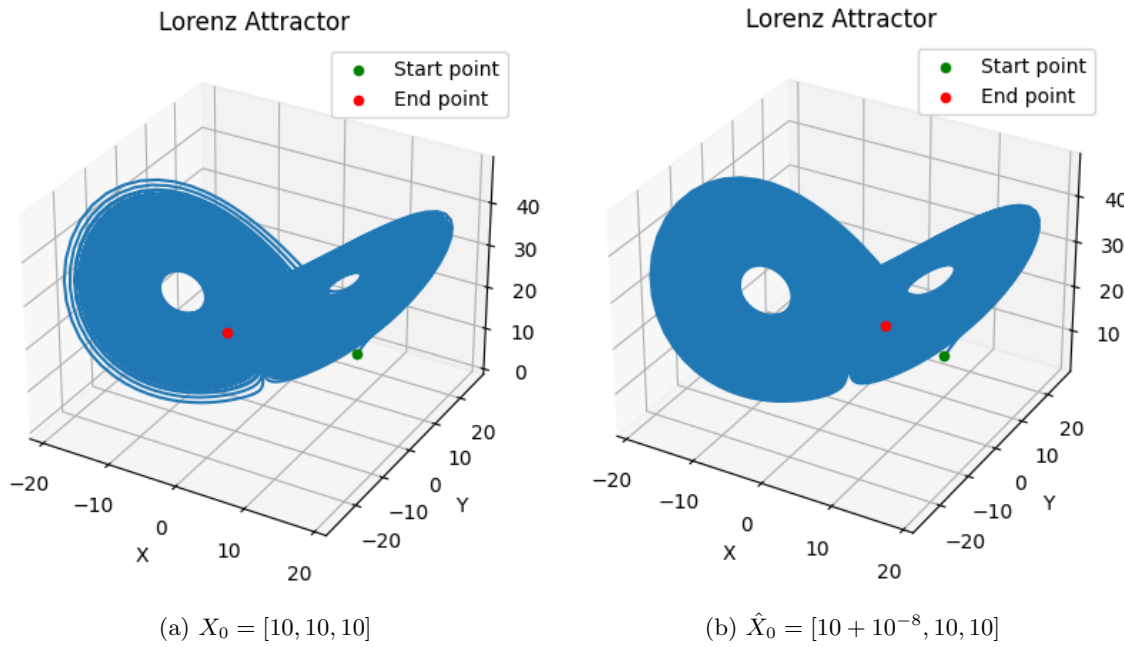


Figure 10: Trajectories for different starting points

- **Effect of small perturbations:** To study the effects of small perturbations, we plot another trajectory, this time starting the system with a very small perturbation from $\hat{X}_0 = [10 + 10^{-8}, 10, 10]$. The rest of the conditions were left the same as previously. The trajectory can be seen in the figure 10b. We can clearly see that a very small change in the initial position leads to completely different ending positions, thus solidifying our conclusion from the previous experiment that no two systems starting from different initial conditions will follow each other's trajectories. We also plotted the difference between the two trajectories ($\|x(t) - \hat{x}(t)\|^2$) shown in figure 11 and recorded the time at which the difference between the two trajectories became larger than 1. From our calculations, we observe that the difference becomes larger than 1 at 24.81 seconds.

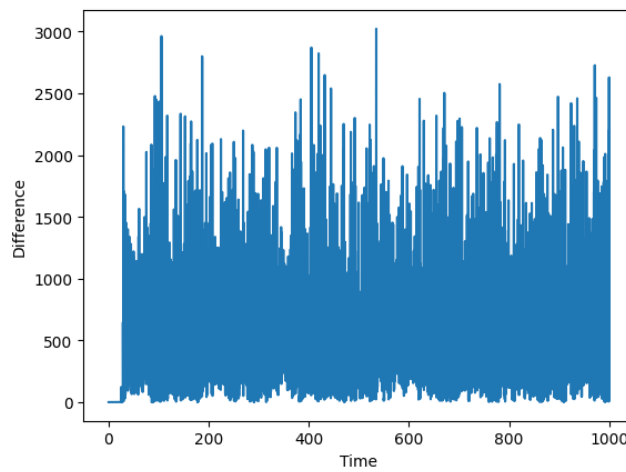
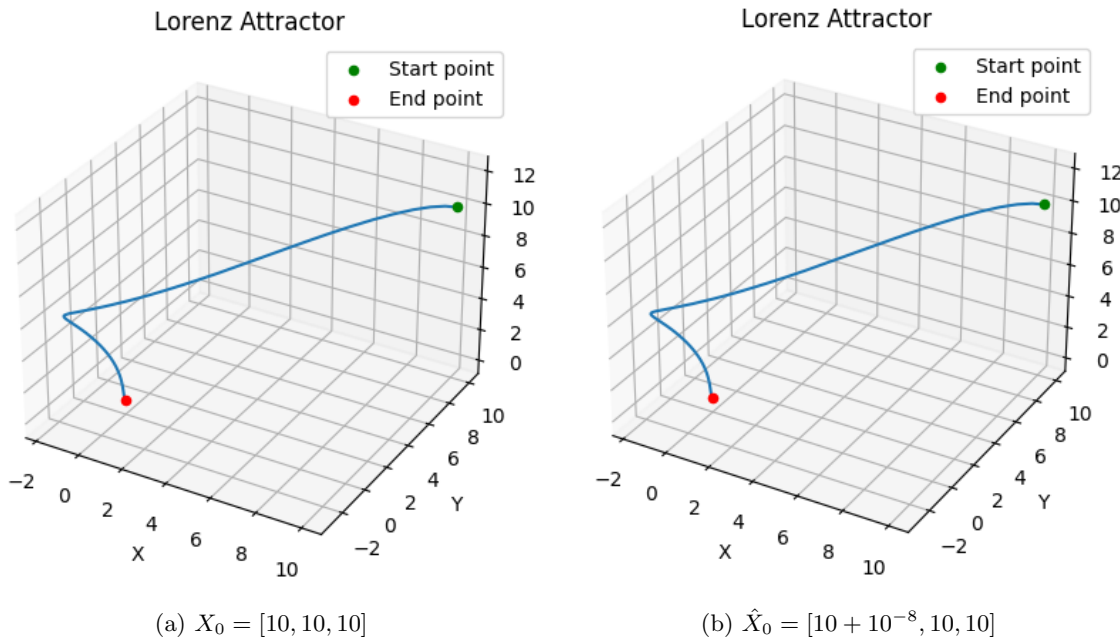


Figure 11: Difference between the two trajectories

- **Effect of $\rho = 0.5$:** We change one of the parameters ρ to 0.5 and plot the two trajectories again shown in figure 12. We can observe that the trajectories are identical and are probably less sensitive to the initial conditions. The trajectories although are very different from when the ρ value was 28, this indicates that a bifurcation (or multiple ones) occur somewhere between these values.

Figure 12: Trajectories for different starting points with $\rho=0.5$

Report on task 5, Bifurcations in crowd dynamics

In this task, we apply bifurcation theory to the SIR model, a commonly used framework in epidemiology for understanding the spread of diseases within a population. The model categorizes the population into three compartments: Susceptible (S), Infected (I), and Recovered (R). Individuals in the susceptible category can contract the disease, becoming infected, and those who are infected will eventually recover, gaining immunity. The transitions between these compartments are governed by a set of differential equations that determine the rate of movement from one compartment to another. Parameters such as the rate of infection and recovery are pivotal in comprehending the disease's spread and how it can be controlled.

- **Part 1,2: Implementation of the SIR Model** To address the task at hand, we have updated the existing `sir_model.py` file to include the missing imports and also equations. So we have successfully implemented the SIR model. The model is characterized by the following system of differential equations:

$$\frac{dS}{dt} = A - \delta S - \frac{\beta SI}{S + I + R}, \quad (5)$$

$$\frac{dI}{dt} = -(\delta + \nu)I + \frac{\beta SI}{S + I + R} - \mu(b, I)I, \quad (6)$$

$$\frac{dR}{dt} = \mu(b, I)I - \delta R. \quad (7)$$

In these equations, S , I , and R denote the susceptible, infected, and recovered populations, respectively. The parameters include the recruitment rate A , the natural death rate δ , the disease-induced death rate ν , the contact rate β , and the recovery rate μ . The recovery rate μ is a function of the infected population I and the number of beds per 10,000 individuals b , defined as:

$$\mu(b, I) = \mu_0 + \frac{(\mu_1 - \mu_0)b}{b + I}. \quad (8)$$

For our simulation, we set the initial time t_0 to the end time t_{end} of 1000. The SIR model parameters were chosen as follows: $\beta = 11.5$, $A = 20$, $\delta = 0.1$, $\nu = 1$, $b = 0.01$ (representing the bed parameter), $\mu_0 = 10$ (minimum recovery rate), and $\mu_1 = 10.45$ (maximum recovery rate).

- Population Dynamics

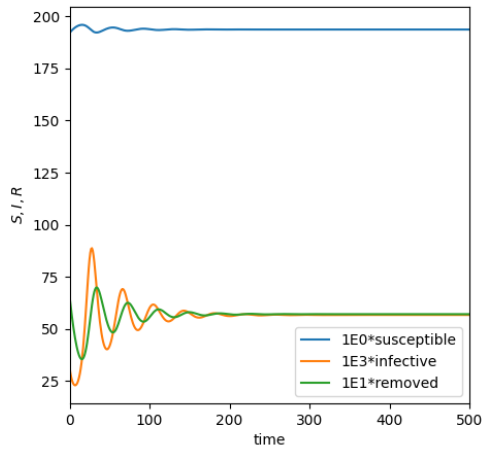


Figure 13: Population dynamics over time

The first plot (figure 13) details the time evolution of the populations:

- * The blue line illustrates the susceptible population (S), scaled by 1×10^0 .
- * The orange line traces the infected population (I), scaled by 1×10^3 .
- * The green line represents the recovered population (R), scaled by 1×10^1 .

Time evolution of a SIR model for disease spread. The blue curve represents the number of susceptible individuals ($10 \times S$), decreasing over time as they become infected. The orange curve illustrates the number of infectious individuals ($10^3 \times I$), initially rising and then falling as the disease progresses. The green curve shows the number of removed individuals ($10 \times R$), including those who have recovered or died, which increases over time. The susceptible population declines without fluctuation, while the infected population shows a rise followed by a decline, and the removed population consistently increases, indicating the progression of recovery or mortality due to the infection.

- Recovery Rate and Infected Population

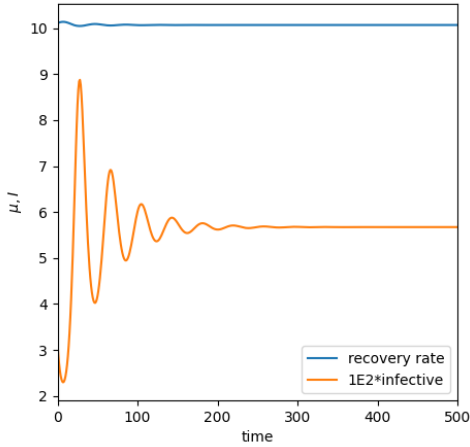


Figure 14: Recovery rate and infected population

The second graph (figure 14) illustrates both the recovery rate (μ) and the infected population:

- * The blue line indicates the recovery rate, which exhibits relative constancy over the observed period.
- * The orange line represents the infected population (I), multiplied by 100 ($100 \times I$), and shows fluctuating behavior with a general trend towards decrease. This is likely caused by the interplay between the fixed transmission rate ($\beta = 11.5$), the periodic recovery rate, and the stochastic initial conditions. The infection rate is determined by the contact rate, which is fixed, and the periodically varying recovery rate introduces non-linear dynamics into the system, resulting in the observed fluctuations. The model assumes a constant population with no births or deaths, except for those due to the disease.

This graph illustrates the complex relationship between the recovery rate and the infected population, suggesting that the recovery rate does not depend solely on the infection numbers.

- Indicator Function

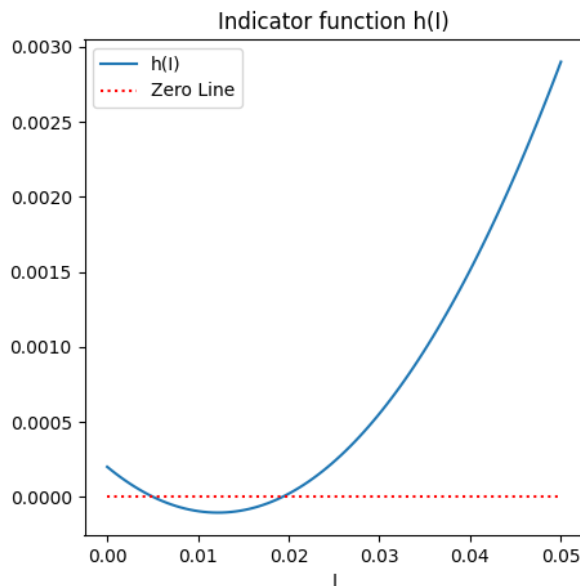


Figure 15: Indicator function $h(I)$

The third graph (figure 15) features the indicator function $h(I)$ plotted against the infected population (I):

- * The blue curve signifies the indicator function $h(I)$, utilized to identify bifurcation points or thresholds within the system.

The indicator function is at zero for a range of I values, which indicates a state of equilibrium. As the value of I increases, $h(I)$ surges, indicating a possible bifurcation or a shift in the system's stability. The reproduction number R_0 is calculated to be approximately 0.9957. The system is globally asymptotically stable if $\beta \leq \delta + \nu + \mu_0$; however, this condition is not met since the inequality evaluates to False. This implies that the system is not asymptotically stable.

- **Part 3: Change of parameter b**

We are set to modify the parameter 'b', which represents the number of beds, to observe a specific bifurcation phenomenon. To achieve this, we will adjust 'b' incrementally from 0.01 to 0.03, in steps of 0.001. This alteration will be applied across three different starting points for the populations: Susceptible (S_0), Infected (I_0), and Recovered (R_0). The chosen initial conditions are $(S_0, I_0, R_0) = (195.3, 0.052, 4.4)$, $(195.7, 0.03, 3.92)$, and $(193, 0.08, 6.21)$. We show the results for the initial point $(195.7, 0.03, 3.92)$ for our discussions in fig 16.

- **b<0.022:** For values of b less than 0.022, we observe the trajectories spiralling inwards towards a specific point over time. This spiralling signals that the populations of susceptible, infectious, and

recovered individuals are stabilizing. This central point acts as an attractor, pulling the system towards a balanced state.

- **b=0.022:** At this value of b, we observe that the system encounters a hopf bifurcation. This leads to the emergence of an oscillatory behaviour with trajectories forming limit cycles indicating periodic oscillations in the infectious population.
- **b>0.022:** At values of b greater than 0.022, the trajectories again approach a stable point, indicating a return to stability. This stable point represents an equilibrium where the infectious disease is effectively controlled.

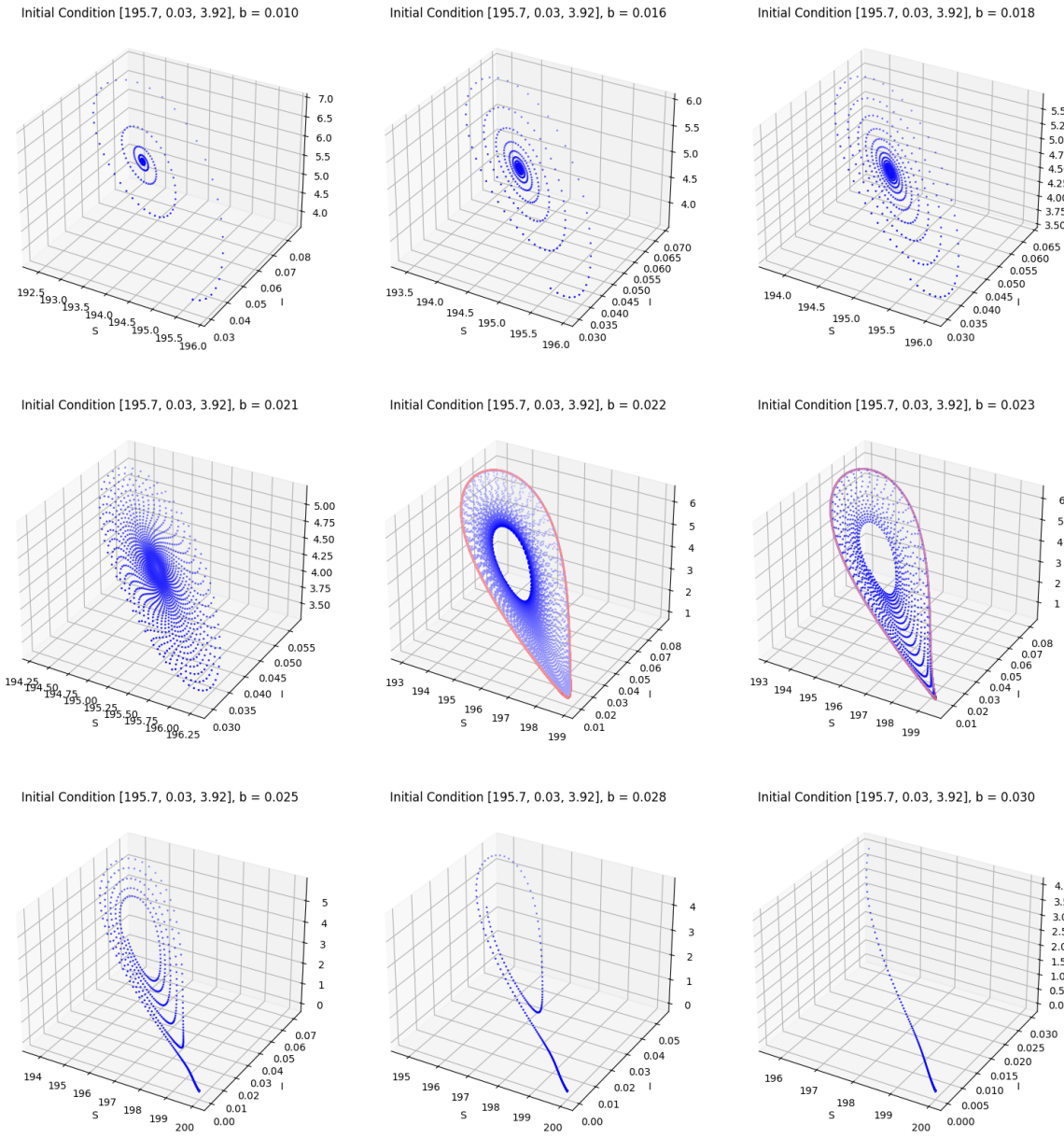


Figure 16: State (195.7, 0.03, 3.92) results

• Part 4: Bifurcation between $b = 0.02$ and $b = 0.03$

Looking at the plots from the previous task, we have already seen that a hopf bifurcation occurs at value of **b=0.022**.

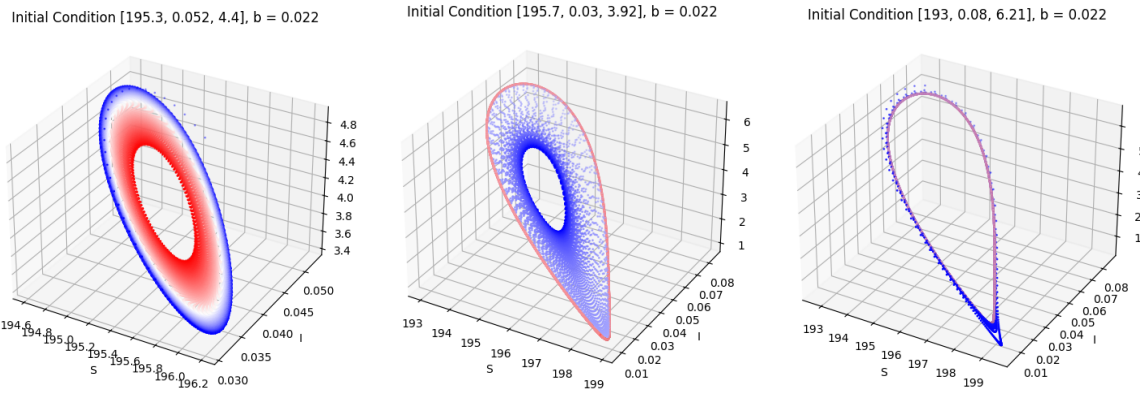


Figure 17: State results

These images in figure 17 show that the system is exhibiting a Hopf bifurcation. A Hopf bifurcation occurs in a dynamical system when a pair of complex conjugate eigenvalues of the linearization around a steady state pass through the imaginary axis in the complex plane. As a result, a limit cycle is created or destroyed, depending on whether the bifurcation is supercritical or subcritical.

The first image shows a closed orbit, which is characteristic of a periodic solution or limit cycle. The second image shows a denser set of points forming a torus, suggesting quasi-periodic behavior on a two-dimensional torus. The third image also shows a closed orbit but with a different shape and size, indicating a change in the system's dynamics.

The normal form of Hopf bifurcation is the same as in specified in the task 3 which can be represented by these equations.

$$\begin{aligned}\dot{x}_1 &= \alpha x_1 - x_2 - x_1(x_1^2 + x_2^2) \\ \dot{x}_2 &= x_1 + \alpha x_2 - x_2(x_1^2 + x_2^2)\end{aligned}$$

where z is a complex variable, λ represents the bifurcation parameter, ω is the frequency of oscillations, and α is a complex constant determining the nature and stability of the bifurcation.

- **Part 5: Reproduction rate R_0**

In the paper, the reproduction rate R_0 is defined in equation (3.1) as follows:

$$R_0 = \frac{\beta}{d + \nu + \mu_1}$$

Here, β represents the average number of adequate contacts per unit of time with infectious individuals, d is the per capita natural death rate, ν is the per capita disease-induced death rate, and μ_1 is the maximum per capita recovery rate due to sufficient healthcare resources and the inherent property of a specific disease.

When the parameter β increases, it implies more frequent contacts that can potentially lead to infection, thus increasing the reproduction rate R_0 . A higher R_0 means that each infected person is likely to infect more people, leading to a more rapid spread of the infection. Conversely, if β decreases, it leads to fewer contacts and a lower reproduction rate R_0 , reducing the spread of the infection.

The relationship between the transmission rate β and the reproduction rate R_0 is visually represented in Figure 18, where it can be observed that as β increases, so does R_0 . The critical threshold for R_0 is depicted as a horizontal line at $R_0 = 1$, below which the disease is expected to die out, and above which an epidemic can occur.

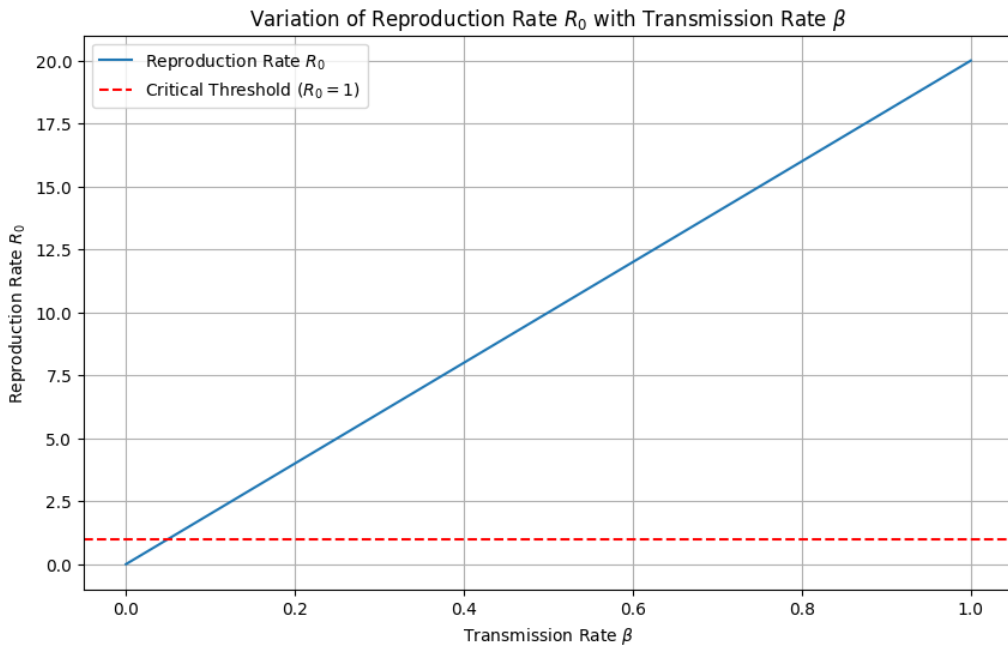


Figure 18: Variation of Reproduction Rate R_0 with Transmission Rate β . The solid blue line represents the reproduction rate as a function of β , and the dashed red line indicates the critical threshold where $R_0 = 1$.

Furthermore, the bifurcation diagram in Figure 19 illustrates the existence of an endemic equilibrium when $R_0 > 1$, which is possible for higher values of β . The blue line indicates that for β values below a critical point, there is no endemic equilibrium and the disease-free state is stable, as shown by the black dot.

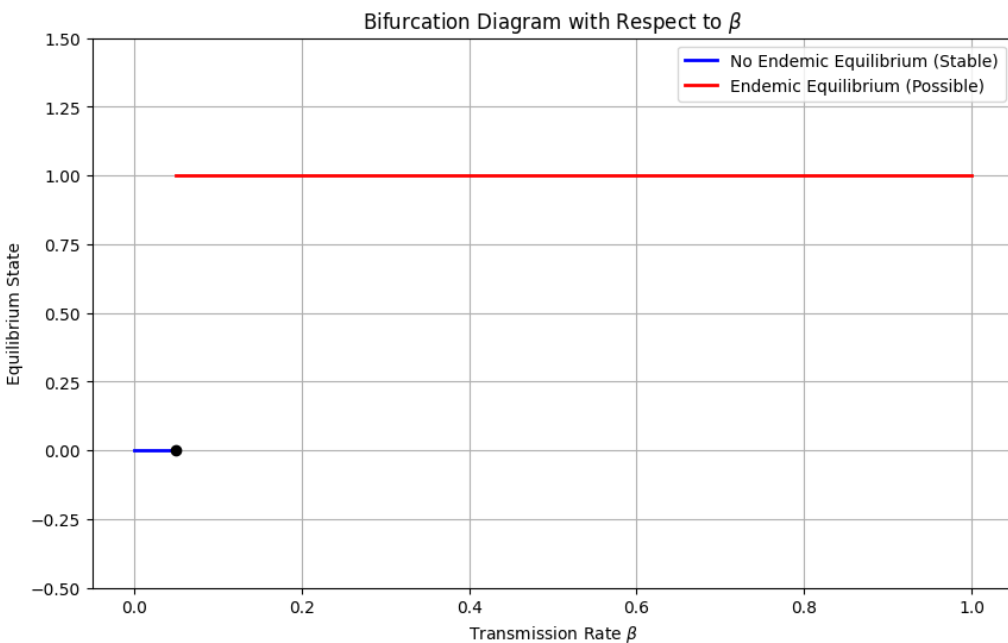


Figure 19: Bifurcation Diagram with respect to β . The solid red line shows the range of β values for which the endemic equilibrium exists, and the blue line and dot represent the disease-free equilibrium state.

- **Part 6: Attractive node**

The behavior described by Theorem 3.2 [4] is confirmed by the numerical simulations depicted in Figure 20. As shown, regardless of initial conditions, the trajectories for susceptible (S), infected (I), and recovered (R) individuals converge to the disease-free equilibrium E_0 , which is indicated by the grey dashed line. This convergence is consistent with the theorem's assertion that E_0 is an attracting node for $R_0 < 1$.

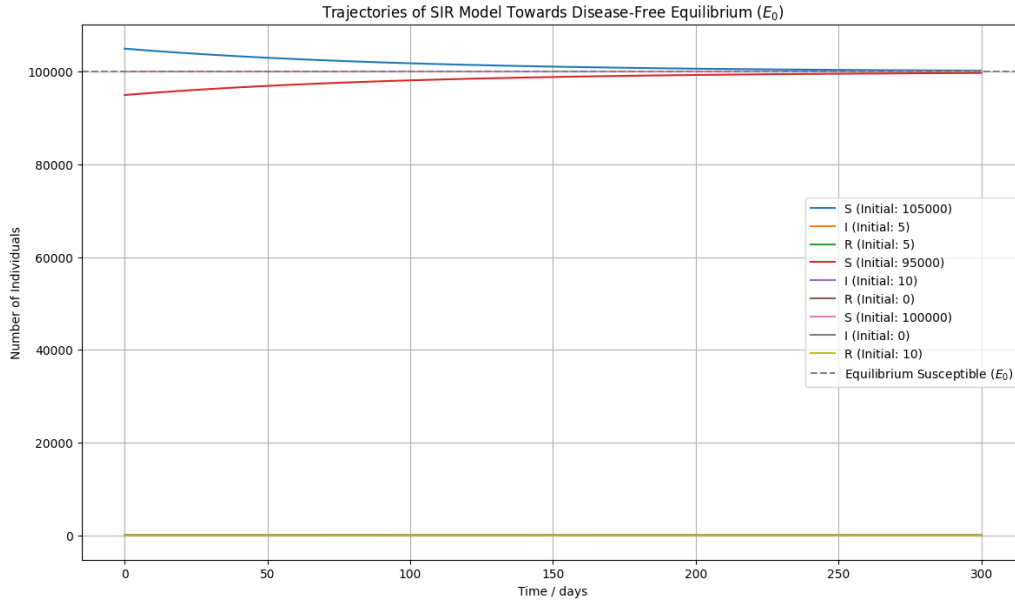


Figure 20: Trajectories of SIR Model Towards Disease-Free Equilibrium (E_0). The convergence of the trajectories to E_0 for different initial conditions illustrates that the equilibrium is an attracting node, following Theorem 3.2.

- **Part 7: Bonus**

Backward bifurcation is a type of bifurcation in which an endemic equilibrium point exists even when the basic reproduction number R_0 is less than 1. Usually, this means, that the disease will die out. However, for backward bifurcation, the disease can persist in the population.

To implement backward bifurcation, we created the function `model_with_backward_bifurcation`. The function almost looks the same as the previously used `model` function. The only difference occurs in the calculation of the variable `dIdt`. We add a backward bifurcation term: `epsilon * I ** 2`. Epsilon is an additional parameter the function takes which should be set to a small positive number. Since the term only depends on epsilon and I, the difference between Hopf bifurcation and backward bifurcation becomes visible once these parameters, especially I, are big enough. In figure 21, we used $I = 0.52$ and $\epsilon = 0.01$.

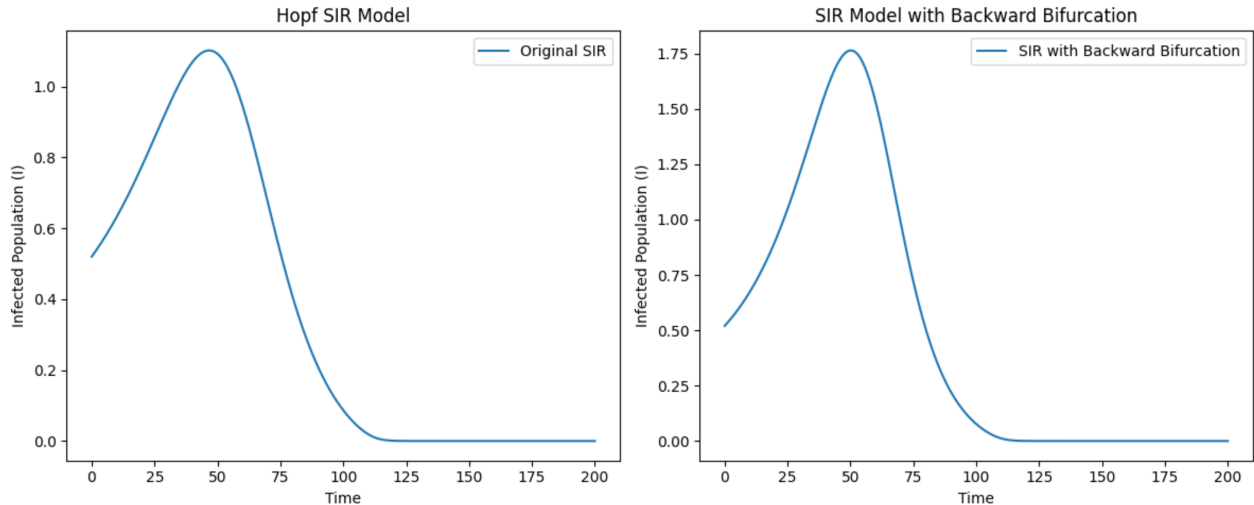


Figure 21: Comparison of the Hopf and backward bifurcation models

For the Hopf SIR Model, a nearly constant increase in the infected population can be seen with a maximum at time step 50 of about $I = 1.1$. The value afterward declines until it reaches zero at time step 112. In comparison, the backward bifurcation model shows a slight exponential increase up to a maximum of $I = 1.75$ just a bit after time step 50. Despite a higher maximum, the model seems to reach a value of zero four time steps earlier.

The behavior observed in the backward bifurcation model highlights the complex dynamics of disease transmission and control. It underscores the importance of considering non-linear effects in epidemiological modeling, particularly for diseases with atypical transmission characteristics. The choice of model parameters, including ϵ , should be informed by the specific disease dynamics and empirical data.

References

- [1] Charles R. Harris, K. Jarrod Millman, Stéfan J. van der Walt, Ralf Gommers, Pauli Virtanen, David Cournapeau, Eric Wieser, Julian Taylor, Sebastian Berg, Nathaniel J. Smith, Robert Kern, Matti Picus, Stephan Hoyer, Marten H. van Kerkwijk, Matthew Brett, Allan Haldane, Jaime Fernández del Río, Mark Wiebe, Pearu Peterson, Pierre Gérard-Marchant, Kevin Sheppard, Tyler Reddy, Warren Weckesser, Hameer Abbasi, Christoph Gohlke, and Travis E. Oliphant. Array programming with NumPy. *Nature*, 585(7825):357–362, September 2020.
- [2] J. D. Hunter. Matplotlib: A 2d graphics environment. *Computing in Science & Engineering*, 9(3):90–95, 2007.
- [3] Edward N. Lorenz. Deterministic nonperiodic flow. *Journal of the Atmospheric Sciences*, 20(2):130–141, March 1963.
- [4] Chunhua Shan and Huaiping Zhu. Bifurcations and complex dynamics of an sir model with the impact of the number of hospital beds. *Journal of Differential Equations*, 257(5):1662–1688, 2014.
- [5] Yuri A. Kuznetsov. *Elements of Applied Bifurcation Theory*. Springer New York, 2004.